

The following resources related to this article are available online at www.sciencemag.org (this information is current as of July 9, 2009):

A correction has been published for this article at:

<http://www.sciencemag.org/cgi/content/full/sci;293/5537/1997>

Updated information and services, including high-resolution figures, can be found in the online version of this article at:

<http://www.sciencemag.org/cgi/content/full/293/5529/474>

Supporting Online Material can be found at:

<http://www.sciencemag.org/cgi/content/full/293/5529/474/DC1>

A list of selected additional articles on the Science Web sites **related to this article** can be found at:

<http://www.sciencemag.org/cgi/content/full/293/5529/474#related-content>

This article **cites 31 articles**, 1 of which can be accessed for free:

<http://www.sciencemag.org/cgi/content/full/293/5529/474#otherarticles>

This article has been **cited by** 281 article(s) on the ISI Web of Science.

This article has been **cited by** 18 articles hosted by HighWire Press; see:

<http://www.sciencemag.org/cgi/content/full/293/5529/474#otherarticles>

This article appears in the following **subject collections**:

Atmospheric Science

<http://www.sciencemag.org/cgi/collection/atmos>

Information about obtaining **reprints** of this article or about obtaining **permission to reproduce this article** in whole or in part can be found at:

<http://www.sciencemag.org/about/permissions.dtl>

sensed observations together with a transfer function derived from in situ observations. The net basin-integrated effect of El Niño and La Niña events on the rates of biological production in the equatorial Pacific is significant and plays a strong role in the largest known natural year-to-year perturbation of the global carbon cycle (5, 25, 37). Future observations will provide data to validate the approach on larger spatial scales, extending it to off-equatorial regions and possibly to global scales.

References and Notes

1. R. T. Barber, F. P. Chavez, *Science* **222**, 1203 (1983).
2. F. P. Chavez, R. T. Barber, *Deep-Sea Res.* **34**, 1229 (1987).
3. R. T. Barber, J. E. Kogelschatz, in *Global Ecological Consequences of the 1982-83 El Niño-Southern Oscillation*, P. W. Glynn, Ed. (Elsevier, New York, 1989), pp. 21–53.
4. J. W. Murray, R. T. Barber, M. R. Roman, M. P. Bacon, R. A. Feely, *Science* **266**, 58 (1994).
5. F. P. Chavez et al., *Science* **286**, 2126 (1999).
6. D. Turk, M. R. Lewis, W. G. Harrison, T. Kawano, I. Asanuma, *J. Geophys. Res.* **106**, 4501 (2001).
7. R. W. Eppley, B. J. Peterson, *Nature* **282**, 677 (1979).
8. R. A. Feely, R. Wanninkhof, T. Takahashi, P. Tans, *Nature* **398**, 597 (1999).
9. J. W. Murray, J. N. Downs, S. Storm, C. L. Wei, H. W. Jannasch, *Deep-Sea Res.* **36**, 1471 (1989).
10. M. A. Peña, M. R. Lewis, W. G. Harrison, *Mar. Ecol. Prog. Ser.* **80**, 265 (1992).
11. J. J. McCarthy, C. Garside, J. L. Nevins, R. T. Barber, *Deep-Sea Res.* **43**, 1065 (1996).
12. M. Rodier, R. LeBorgne, *Deep-Sea Res.* **44**, 2085 (1997).
13. P. Raimbault et al., *J. Geophys. Res.* **104**, 3341 (1999).
14. F. P. Wilkerson, R. C. Dugdale, *J. Geophys. Res.* **97**, 669 (1992).
15. M. J. McPhaden et al., *J. Geophys. Res.* **103**, 14169 (1998).
16. J. Picaut, A. J. Busalacchi, in *Radar Altimetry*, L. Fu, A. Cazenave, Eds. (Academic Press, New York, in press).
17. M. J. McPhaden, *Science* **283**, 950 (1999).
18. C. L. Leonard, C. R. McClain, *Int. J. Remote Sensing* **17**, 721 (1996).
19. P. Falkowski, R. T. Barber, V. Smetacek, *Science* **281**, 200 (1998).
20. The 20°C isotherm depth (a proxy for the thermocline depth) was determined from the TOPEX/Poseidon-derived sea surface height based on relationships established from the depth profiles of temperature collected by the TAO buoy array. The altimeter-derived sea level was binned into 10-day averages, with a spatial averaging of 1° × 1° degree. The depth of the 20°C isotherm was derived from eight buoys spread along the equatorial band, and these data were also averaged over the same 10-day interval as used for altimetric heights. The two data sets, covering a time period from 1992 to 2000, were matched with respect to time and space grids. Anomalies in sea level and 20°C depth were then obtained by subtracting the mean seasonal cycle of the sea level and 20°C depth, derived from the period 1993–1996, from the original time series (1992–2000). The mean formulated over this period is representative of the mean as determined from longer data sets of surface wind, sea surface temperature, and tide gauges (32). The depth of the 20°C isotherm across the entire equatorial domain (140°E to 100°W, 1°N to 1°S) for the period 1992–2000 was then calculated by adding the interannual anomalies as determined from TOPEX/Poseidon sea level anomalies to the mean state.
21. The values for depth-integrated new production and coincident thermocline depths were obtained from a variety of sources at different times and locations in the equatorial Pacific band from 1°N to 1°S. These

- included data from 145°E to 165°W during November–December 1994, December 1995–January 1996, January 1997, and December 1997–January 1998 (6); at 155°W for mean conditions, El Niño 1998 onset, El Niño 1998 maturity, and La Niña 1999 (5); at 87°W during June 1988 (9); at 135°W in April 1988 (10); at 140°W in February–March 1992 and August–September 1992 (11); at 167°E in October 1994 (12) (one reported station was removed from the analysis); at 150°W during November 1994 (13); at 150°W in February–March 1988 (14); and at 140°W in March 1992 and October 1992 [(33) with adjustments made in the day length for consistency with the other data]. New production was determined from shipboard measurements of ¹⁵N-labeled nitrate, with the exception of (5), where we use reported primary production and the *f* ratio to determine the rates of new production.
22. D. A. Siegel, D. J. McGillicuddy Jr., E. A. Fields, *J. Geophys. Res.* **104**, 13359 (1999).
23. To evaluate the importance of local upwelling in our analysis, TAO data were used to compute zonal wind stress, assuming a constant drag coefficient (1.2 × 10⁻³) and air density. We calculated 10-day averages of the wind stress around the center dates of the new production data. The stresses were either averaged spatially over the same zonal intervals as the new production sections, or were computed at the longitude of new production data for values derived from a single location. The wind stresses were added to the regression of new production on thermocline depth in a stepwise fashion. The incremental improvement to the explained variance (4%) is not statistically different from zero. The reason for the relative lack of improvement when including local zonal wind stress is that large-scale, remotely wind-forced upwelling, as manifest through thermocline depth variations, is the principal physical process driving vertical fluxes of heat and nutrients into the surface layer, rather than local wind-forced upwelling. The primacy of non-local wind-forced dynamics in affecting large-scale thermocline depth variations and surface layer prop-

- erties is a common feature of most current theories of ENSO (34, 35).
24. B. M. Uz, J. A. Yoder, V. Osychny, *Nature* **409**, 597 (2001).
25. M. J. Behrenfeld et al., *Science* **291**, 2594 (2001).
26. The relative importance of other physical processes, such as meridional advection, local upwelling, salinity variations, and internal wave dynamics, will differ in areas outside the equatorial band. Based on recent observations, we anticipate that although the general form of our model will have wide applicability, the coefficients relating sea level to thermocline height and relating thermocline depth to new production may vary somewhat in different areas.
27. R. Murtugudde, S. Signorini, J. R. Christian, A. J. Busalacchi, C. R. McClain, *J. Geophys. Res.* **104**, 18351 (1999).
28. C. Meinen, M. J. McPhaden, *J. Phys. Oceanogr.*, **31**, 1324 (2001).
29. J. J. Cullen, *Limnol. Oceanogr.* **40**, 1336 (1995).
30. R. C. Dugdale, F. P. Wilkerson, *Nature* **391**, 270 (1998).
31. P. J. Rayner, I. G. Enting, R. J. Francey, R. Lagerfelds, *Tellus* **51B**, 213 (1999).
32. E. C. Hackert, A. J. Busalacchi, R. Murtugudde, *J. Geophys. Res.* **106**, 2345 (2001).
33. P. Wheeler, unpublished Joint Global Ocean Flux Study data (see <http://usjgofs.whoi.edu/jg/dir/jgofs/eqpac/>).
34. D. S. Battisti, *J. Atmos. Sci.* **45**, 2889 (1988).
35. P. S. Schopf, M. J. Suarez, *J. Atmos. Sci.* **45**, 549 (1988).
36. The authors are grateful to T. Mudge and D. McClurg for assistance with data processing and to C. McClain, I. Asanuma, and T. Kawano for insight and opportunities to pursue this research. Financial support was provided by NASA's Mission to Planet Earth Program, the Natural Sciences and Engineering Research Council of Canada, and NOAA's Office of Atmospheric and Oceanic Research.

10 October 2000; accepted 13 June 2001

The Recent Increase in Atlantic Hurricane Activity: Causes and Implications

Stanley B. Goldenberg,^{1*} Christopher W. Landsea,¹ Alberto M. Mestas-Nuñez,² William M. Gray³

The years 1995 to 2000 experienced the highest level of North Atlantic hurricane activity in the reliable record. Compared with the generally low activity of the previous 24 years (1971 to 1994), the past 6 years have seen a doubling of overall activity for the whole basin, a 2.5-fold increase in major hurricanes (≥50 meters per second), and a fivefold increase in hurricanes affecting the Caribbean. The greater activity results from simultaneous increases in North Atlantic sea-surface temperatures and decreases in vertical wind shear. Because these changes exhibit a multidecadal time scale, the present high level of hurricane activity is likely to persist for an additional ~10 to 40 years. The shift in climate calls for a reevaluation of preparedness and mitigation strategies.

During 1970–1987, the Atlantic basin experienced generally low levels of overall tropical cyclone activity. The relative lull was manifested in major hurricane (*I*) activity (Fig. 1), major hurricane landfalls on the East Coast of the United States and overall hurricane activity in the Caribbean. A brief resurgence of activity in 1988 and 1989 made it

appear that the Atlantic basin was returning to higher levels of activity similar to the late 1920s through the 1960s (2). This notion was later discarded when the activity returned to lower levels from 1991–1994 (3), due in part to the long-lasting (1990–1995) El Niño event (4). This event ended in early 1995 and was followed later that year by one of the

REPORTS

most active Atlantic hurricane seasons on record (5). Activity has been well above average each year since 1995, except for 1997. Here we address the question of whether or not the increase in activity reflects a long-term climate shift, as suggested by previous studies (6–9), and provide evidence that confirms this suggestion based on changes in oceanic and atmospheric conditions.

The North Atlantic basin (including the North Atlantic Ocean, the Caribbean Sea, and the Gulf of Mexico) exhibits substantial interannual and interdecadal variability of tropical cyclone activity. This variability is especially pronounced in major hurricane activity. Interdecadal major hurricane fluctuations occur in both landfall locations (10) and overall activity (11–13). Most of the deadliest and

costliest Atlantic tropical cyclones (10) are major hurricanes. Major hurricanes account for just over 20% of the tropical storms and hurricanes that strike the United States but cause more than 80% of the damage (14).

Most Atlantic tropical cyclones form from atmospheric easterly (African) waves that propagate westward from Africa across the tropical North Atlantic and Caribbean Sea, primarily between 10° and 20°N [termed the “main development region” (MDR) (15, 16) (see Fig. 2A)]. The Atlantic tropical cyclones not spawned by African waves usually form poleward of 25°N. African waves account for ~60% of the Atlantic basin tropical storms and nonmajor hurricanes but ~85% of major hurricanes (17). Almost all major hurricanes formed from African waves begin development (i.e., attain tropical depression status) in the MDR (15) and, thus, are more sensitive to climatic fluctuations in the tropics.

Although the number of easterly waves in the tropical Atlantic is fairly constant from year to year, the fraction that develop into tropical cyclones varies substantially (18, 19). The key to understanding the fluctuations on interannual and interdecadal scales is the MDR. The climat-

ic forcing that affects that region can be separated into local and remote factors. In combination, these factors influence the number of waves that develop into tropical cyclones during each hurricane season. Local factors occur in the actual region and have a direct thermodynamic or dynamic connection to development. Remote factors occur away from the MDR, but are associated (via teleconnections) with conditions in that region. All factors vary on disparate temporal and spatial scales, and there is considerable interdependence between some of them. The extremely active 1995 season, for example, resulted from the juxtaposition of virtually all of the factors known to favor development (5). Among the local tropical Atlantic factors are the lower stratospheric Quasi-Biennial Oscillation (20, 21), sea-level pressure (5, 20, 22), lower tropospheric moisture (5), sea-surface temperature (SST) (23–25), and vertical shear of the horizontal environmental wind (15, 26). The two local factors addressed here are SST and vertical shear.

In general, when looking for long-term variability, it is necessary to look at the oceans because their large thermal and mechanical inertia provide long-term memory and predictability (27). The oceans are the primary energy source for tropical cyclones. Localized SSTs play a direct role in providing moist enthalpy to power incipient tropical cyclones (5, 25). Warmer SSTs decrease atmospheric stability, which increases the penetration depth of a vortex, thus, making developing tropical cyclones more resistant to vertical wind shear (28). Local SST greater than 26.5°C is usually considered to be a necessary condition for tropical cyclone development (26), and higher SST can increase overall activity (23–25). Multidecadal variations in major hurricane activity have been attributed to changes in the SST structure in the Atlantic (2, 12, 13) because tropical North Atlantic SSTs correlate positively with major hurricane activ-

¹National Oceanic and Atmospheric Administration/Atlantic Oceanographic and Meteorological Laboratory/Hurricane Research Division, Miami, FL 33149, USA. ²Cooperative Institute for Marine and Atmospheric Studies/University of Miami, Miami, FL 33149, USA. ³Colorado State University, Department of Atmospheric Sciences, Fort Collins, CO 80523, USA.

*To whom correspondence should be addressed. E-mail: Stanley.Goldenberg@noaa.gov

Fig. 1. Number of major hurricanes from 1944 through 2000 (32). Less reliable data before routine aircraft reconnaissance dictate caution in the use of these data before 1944 (33). Solid horizontal reference line corresponds to sample mean (2.3). Dashed curved line is 5-year running mean. Also shown is the threshold of three major hurricanes per year (dashed straight line).

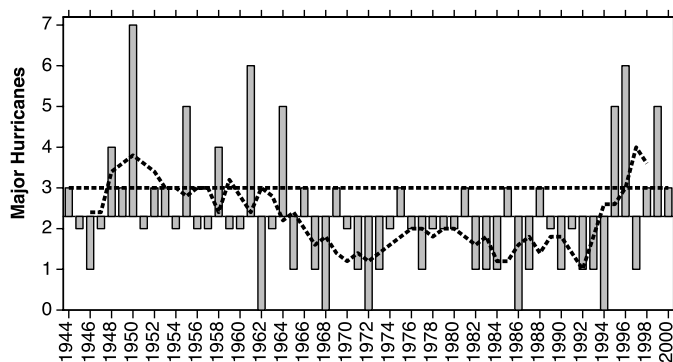
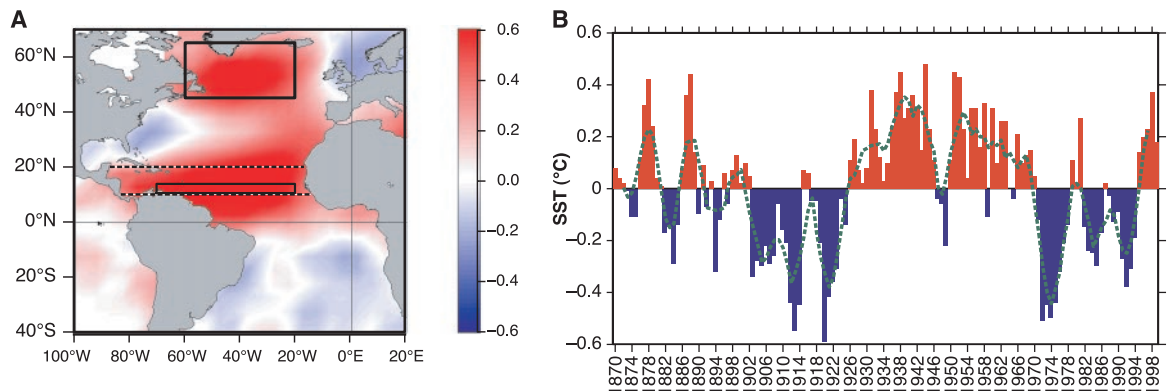


Fig. 2. Atlantic sector of the first rotated EOF of non-ENSO global SST variability for 1870–2000 referred to as the “Atlantic multidecadal mode” (38, 39). (A) Spatial distribution of correlations between local monthly SST anomalies and the modal reconstruction over the indexed region (northern rectangle), the general area where the mode amplitude is the strongest. This distribution has a similar spatial structure to the actual rotated EOF and gives a measure of the local fractional variance (squared temporal correlation) accounted for at each grid point. Dashed lines give north and south boundaries of main development region (MDR) and box (10° to 14°N, 20° to 70°W) is region used to calculate data for Fig. 3. (B) Temporal reconstruction (annual means) of the mode-related variability averaged over the



rectangular areain (A). Dashed curved line is 5-year running mean. Although the signal is stronger in the North Atlantic, it is global in scope with positively correlated co-oscillations in parts of the North Pacific (55). For the multidecadal variations shown here, the coherence between the MDR and far North Atlantic is a robust feature. The SST fluctuations in the far North Atlantic could be used as a proxy for changes in the MDR.

ity. Although North Atlantic SSTs directly impact tropical cyclone activity as a local thermodynamic effect, it appears unlikely that this is their only physical link to hurricane activity. For influencing activity on interannual time scales, this local effect plays either a negligible role (for major hurricanes) or at best a secondary role (for all hurricanes) (24).

The dominant local factor for tropical cyclone activity is the magnitude of the vertical shear of the horizontal wind between the upper and lower troposphere, $|V_z|$. Strong V_z inhibits the formation and intensification of tropical cyclones [e.g., (15, 26)], primarily by preventing the axisymmetric organization of deep convection. Local $|V_z| > \sim 8 \text{ m s}^{-1}$ is generally unfavorable for development (29). The climatological mean vertical wind shear, V_z , for August–September–October (ASO), the peak 3 months of the Atlantic hurricane season during which virtually all major hurricanes form, is westerly with a magnitude $|V_z|$ greater than 8 m s^{-1} over much of the basin (15, 16). Climatologically high values for $|V_z|$ are one of the main reasons why conditions in the Atlantic basin are not especially conducive to tropical cyclone development. The tropical North Atlantic SST appears to act in concert with the overlying tropospheric circulation such that warmer SSTs correspond to reduced $|V_z|$ in the MDR (12, 24).

A key remote factor is SST variability in the central and eastern equatorial Pacific Ocean associated with El Niño–Southern Oscillation (ENSO). Positive Pacific SST anomalies associated with warm-phase ENSO (El Niño) have been linked to increased $|V_z|$ over the MDR, and conversely for cool-phase ENSO (La Niña) (15, 20, 30). Another remote factor that has been linked to interannual and multidecadal variability in Atlantic basin tropical cyclone activity is rainfall variability over the western Sahel (2, 31), with positive rainfall anomalies associated with reduced $|V_z|$ over the MDR (15).

The most obvious indicator of a possible long-term shift are the changes in the tropical cyclone activity itself. The total number of tropical storms and nonmajor hurricanes in the North Atlantic basin has remained fairly constant from decade to decade (13). The numbers of major hurricanes and of Caribbean hurricanes, however, exhibit strong multidecadal variability. The late 1920s to the 1960s were very active, while both the 1900s through mid-1920s and the 1970s through the early 1990s were quiescent (2, 12, 13).

The events of each year reflect a combination of temporal scales. Interannual fluctuations in activity occur in both high and low activity periods (Fig. 1). However, inhibitory influences during relatively inactive multidecadal periods set a limit on the possible level of activity. During 1944–1970 (the portion of the previous active multidecadal period shown in Fig. 1), the average number of major hurricanes per year

was 2.7 (32–34). Six of the years produced four or more major hurricanes. In contrast, the average for the quieter period of approximately equal duration, 1971–1994, was only 1.5, with no years having more than three major hurricanes. The quieter period’s threshold of three major hurricanes was then exceeded in 1995 for the first time since 1964. The average number of major hurricanes for 1995–2000 is 3.8 (34). Three of those years had four or more. The Net Tropical Cyclone activity (NTC) for the North Atlantic, another measure of activity (8), shows a similar combination of interannual and multidecadal fluctuations (35). The only year since 1995 with below average activity was 1997, when the Atlantic hurricane activity was suppressed by the strongest El Niño event of this century (36). Even with 1997 included, the mean number of major hurricanes and mean NTC for 1995–2000 are the highest of any consecutive 6 years in the 1944–2000 record. While this recent period spans only 6 years, it clearly belongs to a different low-frequency climate regime than the previous 24 years (1971–1994).

Studies of global SSTs using empirical orthogonal function (EOF) analysis [e.g., (37)] have shown that the primary source of interannual SST variability is the ENSO region. To analyze the relation of Atlantic tropical cyclone activity with Atlantic SST anomalies in a way that is independent of ENSO, it is helpful to first remove the teleconnected effects of ENSO on the Atlantic Ocean (38). The first rotated non-ENSO SST mode (39) represents interannual to multidecadal variability (Fig. 2). Because the mode’s temporal variability is dominated by multidecadal-scale fluctuations (Fig. 2B) with the largest amplitudes in the Atlantic, we refer to it as the “Atlantic multidecadal mode.” The positive phase of the mode’s spatial pattern (Fig. 2A) has warm SSTs in the tropical North Atlantic from 0° to 30°N (which includes the MDR) and in the far North Atlantic from 40° to 70°N . This mode is not local to the MDR; it is instead a large-scale feature that, because it is also present in the MDR, affects Atlantic tropical cyclone activity. The primary region for SST anomalies that would affect tropical cyclones directly would be in and just north of the MDR, i.e., $\sim 10^\circ$ to 25°N (24, 40).

These multidecadal-scale fluctuations in SSTs closely follow the long-term fluctuations in Atlantic tropical cyclone activity (13). The time series for the Atlantic multidecadal mode (Fig. 2B), major hurricanes (Fig. 1) and NTC (35) all show similar multidecadal-scale shifts. Ignoring interannual fluctuations, major hurricane activity is high from 1944 through at least ~ 1964 (Fig. 1), NTC is high through ~ 1969 (35) and the Atlantic multidecadal mode is predominantly warm until ~ 1970 (Fig. 2B). Then, major hurricane activity and NTC are mostly below average and the Atlantic multidecadal mode colder from the early 1970s through the

early 1990s. All three quantities have increased dramatically since 1995. Note also that the two busiest periods in the 1970s and 1980s, 1979–1981 and 1988–1990 (35), coincide with two short warming periods, 1979–1981 and 1987–1990 (see Fig. 2B), indicating the possibility of significant relations on shorter (decadal) time scales. The correlations between the 5-year running mean of the Atlantic multidecadal mode with the major hurricane and NTC running means are 0.72 and 0.81, respectively (41).

It has been hypothesized that multidecadal changes in oceanic temperatures, major hurricane activity and Sahel rainfall are related to fluctuations in the intensity of the thermohaline circulation in the North Atlantic (12, 42). A faster thermohaline circulation is suggested to be associated with warmer SSTs in the North Atlantic and colder SSTs in the South Atlantic. These conditions would enhance Sahel rainfall and decrease $|V_z|$ in the MDR. In other words, the decadal-scale SST fluctuations affecting Atlantic hurricane (particularly major hurricane) activity would likely produce the connection via changes in the upper- and lower-level zonal atmospheric circulations over the MDR (40). It is also possible, but less likely, that the changes in atmospheric circulation are forcing the SST changes. However, it is doubtful that long-term increased tropical cyclone activity could cause warmer North Atlantic SSTs since hurricanes result in a cooling of SSTs through vertical mixing and upwelling (e.g., 43).

Figure 3 shows the fluctuations in $|V_z|$ averaged for ASO for the south-central portion of the MDR where the strongest correlations between $|V_z|$ and major hurricanes occur (15, 16). Although there is substantial interannual variability in $|V_z|$, primarily associated with ENSO, this is being modulated by the obvious multidecadal-scale fluctuations. These fluctuations show a switch from conducive (high percentages of low $|V_z|$) to suppressed (low percentages of low $|V_z|$) conditions in 1970, almost coincident with the shift in major hurricanes (Fig. 1), NTC (35) and SSTs (Fig. 2B). In Fig. 3, however, the switch back to conducive conditions appears to start in 1988 (44), 7 years earlier than the switch for the other parameters. Even though 1991 through 1994 exhibit a short-term return to less conducive values, 1988 through 1990 had the most favorable values since 1969. Figure 2 shows some evidence of North Atlantic SST warming for a few years around 1988 followed by several cooler years in the early 1990s before the major warming in 1995. The warming around 1988 is much more evident in the Atlantic multidecadal mode values for ASO and in the actual ASO SSTs for the MDR (not shown). Nonetheless, the dominant shift to warmer values clearly takes place in 1995, which is when occurrences of more than three major hurricanes and hyperactive years [$\text{NTC} \geq 150\%$; (35)] resumed.

For almost every measure of tropical cy-

REPORTS

clone activity, the differences between the warm and cold phases of the mode are statistically significant (34, 44). The single exception is the number of U.S. Gulf Coast landfalling major hurricanes. This is because the Gulf of Mexico activity does not have a significant relationship with $|V_z|$ fluctuations in the MDR (11, 12, 15) or to the multidecadal North Atlantic SST fluctuations (Fig. 2A). The greatest differences (ratios) are for major hurricanes, hurricane days, U.S. East Coast major hurricane landfalls, and especially Caribbean hurricanes and U.S. damage. The Caribbean Sea has shown dramatic changes in hurricane activity—averaging 1.7 occurrences per year during the warm periods compared with only 0.5 per year during the cold period (34). The current warm period has produced an average of 2.5 occurrences per year with an unprecedented (since 1944) six hurricanes in the region during 1996. These multidecadal changes are illustrated in Fig. 4, which clearly shows the enhancement of overall Caribbean hurricane activity during warmer periods. Not only is the entire Caribbean region much less active during the colder period (Fig. 4A), but the only hurricanes that

developed during that period in the Caribbean Sea east of $\sim 73^\circ\text{W}$ formed during the two intermittent short warming periods (1979–1981 and 1987–1990) discussed earlier. Large multidecadal fluctuations of major hurricane landfalls are especially evident for the U.S. East Coast from the Florida peninsula to New England and are illustrated in Fig. 5. No major hurricanes made landfall from 1966–1983. This relatively quiet period was similar to, but more extreme than, the low activity period during the first two decades of the 20th century. In contrast, during 1947–1965, 14 major hurricanes struck the East Coast (13). Overall, the United States has experienced about five times as much in median damages from tropical storms and hurricanes during the warm (high activity) than during the cold (low activity) phases of the Atlantic multidecadal mode (44).

The Atlantic tropical cyclone record, which (except for U.S. landfall data) is not considered reliable before 1944 (33), shows less than one complete cycle of the multidecadal signal. The record for the SST signal represented by the Atlantic multidecadal mode (Fig. 2B), however, which has demonstrated a robust relation to the

observed activity, shows about two complete cycles—with some proxy records extending back several additional cycles (42). In addition, U.S. landfall data are able to show almost two periods of the signal (13, 44). Because of the multidecadal scale of the Atlantic SST variability portrayed here, the shift since 1995 to an environment generally conducive to hurricane formation—warmer North Atlantic SSTs and reduced vertical wind shear—is not likely to change back soon (45). This means that during the next 10 to 40 years or so, most of the Atlantic hurricane seasons are likely to have above average activity, with many hyperactive, some around average, and only a few below average. Furthermore, consistent with experience since the active phase began in 1995, there would be a continuation of significantly increased numbers of hurricanes (and major hurricanes) affecting the Caribbean Sea and basin-wide numbers of major hurricanes. The Gulf of Mexico, however, is expected to see only minor differences. Tragic impacts of the heightened activity have already been felt, especially in the Caribbean [e.g., Hurricanes Georges and Mitch (46)]. In addition, an increase in major hurricane landfalls affecting the U.S. East Coast is anticipated, but has not yet materialized (47).

One may ask whether the increase in activity since 1995 is due to anthropogenic global warming. The historical multidecadal-scale variability in Atlantic hurricane activity is much greater than what would be “expected” from a gradual temperature increase attributed to global warming (5). There have been various studies investigating the potential effect of long-term global warming on the number and strength of Atlantic-basin hurricanes. The results are inconclusive (48). Some studies document an increase in activity while others suggest a decrease (49). Tropical North Atlantic SST has exhibited a warming trend of $\sim 0.3^\circ\text{C}$ over the last 100 years (38); whereas Atlantic hurricane activity

Fig. 3. Percentage of south-central portion ($10^\circ\text{--}14^\circ\text{N}$, $20^\circ\text{--}70^\circ\text{W}$) of the main development region (see Fig. 2A) where $|V_z| < 6 \text{ m s}^{-1}$ (values extremely conducive for tropical cyclone development) for ASO. Dashed curved line is 5-year running mean. Higher and lower percentages indicate conditions that are more or less conducive to development, respectively.

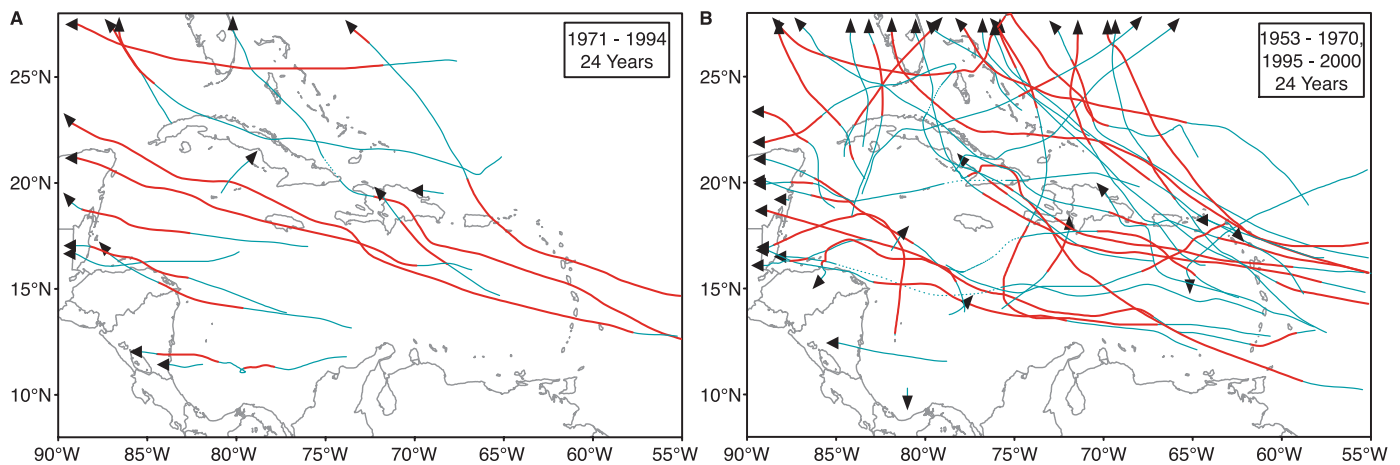
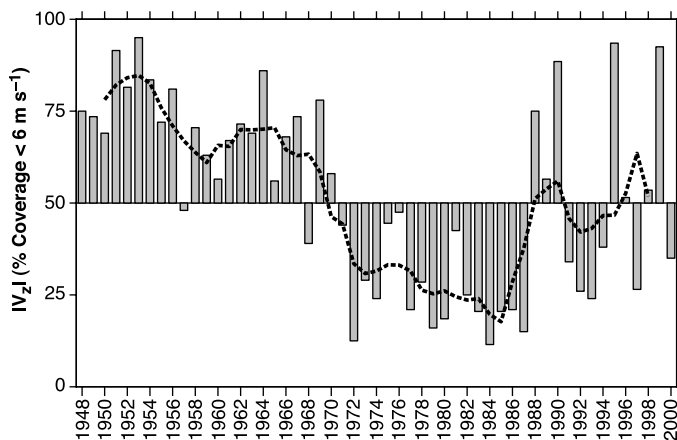
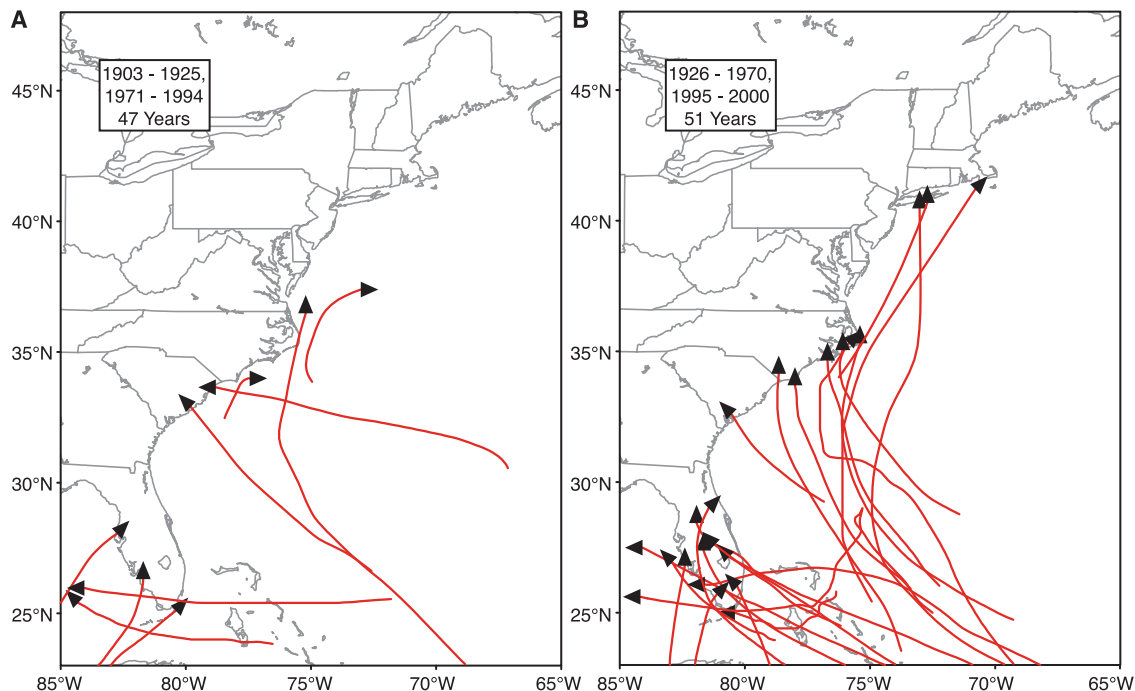


Fig. 4. Contrast of Caribbean hurricanes between colder (A) and warmer (B) values of the Atlantic multidecadal mode. The solid green (thin) and red (thick) lines indicate where the hurricanes were at nonmajor and major hurricane intensities, respectively. Tropical storm intensity is indicated by dotted lines in cases where a hurricane weakened to tropical

storm strength and then re-intensified to hurricane status. The years are similar to (34) except that the first nine warmer years (1944–1952) are not included to make the number of colder and warmer years equal. The colder years (24 years) include 1971–1994. The warmer years (24 years) include 1953–1970 and 1995–2000.

Fig. 5. Contrast of U.S. East Coast major hurricane landfalls between colder (A) and warmer (B) values of the Atlantic multidecadal mode. The solid red lines indicate where the storms were at major hurricane intensity. The years are like those in (44) except that the first four warmer years (1899–1902) are not included to make the number of colder and warmer years similar. Colder years (47 years) include 1903–1925 and 1971–1994. Warmer years (51 years) include 1926–1970 and 1995–2000.



has not exhibited trendlike variability, but rather distinct multidecadal cycles as documented here and elsewhere (12, 13, 17). The extreme activity in 1995 has been attributed in part to the record-warm temperatures in the North Atlantic (25). The possibility exists that the unprecedented activity since 1995 is the result of a combination of the multidecadal-scale changes in Atlantic SSTs (and vertical shear) along with the additional increase in SSTs resulting from the long-term warming trend. It is, however, equally possible that the current active period (1995–2000) only appears more active than the previous active period (1926–1970) due to the better observational network now in place. During the previous active period, only 1966–1970 had continual satellite coverage (33, 50). Further study is essential to separate any actual increase from an apparent one due to more complete observations.

Although increased activity during a particular year does not automatically mean increased storm-related damages (51), years with high activity have a greater overall potential for disaster than years with low activity. Increased occurrence combined with dramatic coastal population increases during the recent lull, add up to a potential for massive economic loss (13). In addition, there remains a potential for catastrophic loss of life in an incomplete evacuation ahead of a rapidly intensifying system. Government officials, emergency managers, and residents of the Atlantic hurricane basin should be aware of the apparent shift in climate and evaluate preparedness and mitigation efforts in order to respond appropriately in a regime where the hurricane threat is much greater than it was in the 1970s through early 1990s.

References and Notes

1. The stages of a tropical cyclone [tropical system (warm core) with "closed" surface circulation and organized deep convection] include tropical depression [maximum sustained (1-min) surface wind $< 18 \text{ m s}^{-1}$], tropical storm ($18 \text{ to } 32 \text{ m s}^{-1}$) and hurricane ($\geq 33 \text{ m s}^{-1}$). Hurricanes that have attained a maximum sustained surface wind speed $\geq 50 \text{ m s}^{-1}$ are referred to as major (or "intense") hurricanes (17), corresponding to categories 3, 4, or 5 on the Saffir-Simpson scale (52). The data source used to calculate the tropical cyclone parameters used in this study is the best track file for the Atlantic basin (53) compiled by the National Hurricane Center (NHC) of the Tropical Prediction Center (TPC) of the National Oceanic and Atmospheric Administration (NOAA).
2. W. M. Gray, *Science* **249**, 1251 (1990).
3. C. W. Landsea, N. Nicholls, W. M. Gray, L. A. Avila, *Geophys. Res. Lett.* **23**, 1697 (1996).
4. K. E. Trenberth, T. J. Hoar, *Geophys. Res. Lett.* **23**, 57 (1996).
5. C. W. Landsea, G. D. Bell, W. M. Gray, S. B. Goldenberg, *Mon. Weather Rev.* **126**, 1174 (1998).
6. S. B. Goldenberg, L. J. Shapiro, C. W. Landsea, Preprints, *7th Conference on Climate Variations*, Long Beach CA, 2 to 7 February 1997 (American Meteorology Society, Boston, MA, 1977), pp. 305–310.
7. R. M. Wilson, *Geophys. Res. Lett.* **26**, 2957 (1999).
8. W. M. Gray, C. W. Landsea, P. W. Mielke Jr., K. J. Berry, E. Blake, Summary of 2000 Atlantic tropical cyclone activity and verification of authors' seasonal activity prediction. (Colorado State Univ., Fort Collins, CO, 2000). Available at: <http://tropical.atmos.colostate.edu/forecasts/2000/nov2000/index.html>
9. J. B. Elsner, T. Jagger, X. F. Niu, *Geophys. Res. Lett.* **27**, 1743 (2000).
10. P. J. Hebert, J. D. Jarrell, M. Mayfield, NOAA Tech. Memo., NWS TPC-1, Miami, FL (1996).
11. C. W. Landsea, W. M. Gray, P. W. Mielke Jr., K. J. Berry, *J. Clim.* **5**, 1528 (1992).
12. W. M. Gray, J. D. Sheaffer, C. W. Landsea in *Hurricanes, Climate and Socioeconomic Impacts*, 15 H. F. Diaz, R. S. Pulwarty, Eds. (Springer, Berlin, 1997), pp. 15–53.
13. C. W. Landsea, R. A. Pielke Jr., A. M. Mestas-Nuñez, J. A. Knaff, *Clim. Change* **42**, 89 (1999).
14. R. A. Pielke Jr., C. W. Landsea, *Weather Forecasting* **13**, 621 (1998).
15. S. B. Goldenberg, L. J. Shapiro, *J. Clim.* **9**, 1169 (1996).
16. See Web figure 1 in supplemental material (54).
17. C. W. Landsea, *Mon. Weather Rev.* **121**, 1703 (1993).
18. N. L. Frank, *Mon. Weather Rev.* **103**, 294 (1975).
19. L. A. Avila, R. J. Pasch, J.-G. Jiing, *Mon. Weather Rev.* **128**, 3695 (2000).
20. W. M. Gray, *Mon. Weather Rev.* **112**, 1649 (1984).
21. L. J. Shapiro, *Mon. Weather Rev.* **117**, 2598 (1989).
22. J. A. Knaff, *J. Clim.* **10**, 789 (1997).
23. L. J. Shapiro, *Mon. Weather Rev.* **110**, 1014 (1982).
24. ———, S. B. Goldenberg, *J. Clim.* **11**, 578 (1998).
25. M. A. Saunders, A. R. Harris, *Geophys. Res. Lett.* **24**, 1255 (1997).
26. W. M. Gray, *Mon. Weather Rev.* **96**, 669 (1968).
27. J. P. Peixoto, A. H. Oort, *Physics of Climate* (American Institute of Physics, New York, 1992), pp. 16–17.
28. M. DeMaria, *J. Atmos. Sci.* **53**, 2076 (1996).
29. ———, J.-J. Baik, J. Kaplan, *J. Atmos. Sci.* **50**, 1133 (1993). The exact threshold value for $|V_z|$ that prevents development depends on the method used to calculate $|V_z|$ (i.e., size of area over which it is averaged), the strength of the system itself, and other environmental factors such as the local SST (28). Although in fluid mechanics shear is defined as the cross-stream partial derivative of the velocity, the normal convention in synoptic meteorology is to use the term "vertical shear", V_z , for the difference in velocity between the upper (200 mb) and the lower (850 mb) troposphere without dividing by the distance between the levels, so that the units of V_z are (m s^{-1}) rather than (s^{-1}) or $(\text{m s}^{-1} \text{ km}^{-1})$.
30. L. J. Shapiro, *Mon. Weather Rev.* **115**, 2598 (1987).
31. C. W. Landsea, W. M. Gray, *J. Clim.* **5**, 435 (1992).
32. Landsea (17) documented that strong hurricanes in the 1940s to the 1960s were assigned slightly higher maximum sustained surface wind speeds for a particular minimum central surface pressure than hurricanes from 1970–1991 with the same central pressure. This bias is as high as 5 m s^{-1} for category 4 and 5 hurricanes. At the threshold value for major hurricanes of 50 m s^{-1} , the bias appears to be $\sim 2.5 \text{ m s}^{-1}$. Therefore, consistent with his bias adjustment, 52 m s^{-1} is used for the present study as the threshold for major hurricanes from 1944–1969. This bias adjustment effectively lowers the number of major hurricanes for certain years before 1970 (e.g., the number of major hurricanes for 1969 is reduced from five to three) and reduces the values for other parameters that utilize major hurricane data.

33. Although these data are available since 1851, only the data for the years since 1944, when routine aircraft reconnaissance of Atlantic tropical cyclones began, are considered very reliable. The greatest reliability starts around the mid-1960s when operational satellite detection of Atlantic tropical cyclones began (50). Before satellite coverage, a portion of the lifetimes of many systems had probably been missed.

34. See Web table 1 in supplemental material (54).

35. See Web figure 2 in supplemental material (54).

36. G. D. Bell, M. S. Halpert, *Bull. Am. Meteorol. Soc.* **79**, 51 (1998).

37. C. K. Folland, J. A. Owen, M. N. Ward, A. W. Colman, *J. Forecasting* **10**, 21 (1991). EOF analysis is a multivariate statistical technique commonly used in climate studies. It allows one to capture the main spatial and temporal variability of climate variables as a few "empirical modes." These modes, however, do not always represent physical modes.

38. D. B. Enfield, A. M. Mestas-Nuñez, *J. Clim.* **12**, 2719 (1999). They represented ENSO as the leading complex EOF of global 1856–1991 SST anomalies in the interannual (1.5 to 8 year) band. Contrary to conventional EOF analysis, complex EOF analysis allows accounting for phase propagation in a single mode. The ENSO mode and a linear trend were then removed from the SST anomalies and an EOF analysis was used to study the residual (non-ENSO) variability.

39. A. M. Mestas-Nuñez, D. B. Enfield, *J. Clim.* **12**, 2734 (1999). They applied an orthogonal rotation to the first 10 global non-ENSO EOFs (38) to investigate the presence of regionalized centers of variability. Rotated EOFs are generally less sensitive to sampling errors than conventional EOFs and thus may be better indicators of physical modes.

40. F. Vitart, J. L. Anderson, *J. Clim.* **14**, 533 (2001). They performed tests with an atmospheric general circulation model to determine if the SST anomalies in the lower (~0°–40°N) or higher (40°–60°N) latitude Atlantic are most responsible for multidecadal scale variations in tropical cyclone activity. The results strongly suggest that the contributions are only from the lower latitude SST anomalies. Their study also attributes at least a portion of the impact to changes in the vertical shear associated with the warmer SSTs.

41. These correlations are statistically significant with greater than 90 and 95% confidence, respectively, using a significance test which accounts for serial correlation. R. E. Davis, *J. Phys. Oceanogr.* **6**, 247 (1976).

42. T. L. Delworth, M. E. Mann, *Clim. Dyn.* **16**, 661 (2000).

43. L. K. Shay, R. L. Elsberry, P. G. Black, *J. Phys. Oceanogr.* **19**, 649 (1989).

44. See Web table 2 in supplemental material (54).

45. Instrumental and proxy data (1650 A.D. to present) as well as model simulations suggest that Atlantic multidecadal variability deviates significantly from a simple stochastic process (42). This evidence also indicates that the signal is broad band (30 to 70 years) and not a single peak in the spectrum. With a broad-band signal it is difficult to predict when sign changes will occur. Due to its multidecadal nature, however, it is reasonable to say that if the signal has recently changed sign, it will probably not change back soon.

46. R. J. Pasch, *Weatherwise* **52**(no. 2), 48 (1999).

47. See "Persistent East Coast trough" in supplemental material (54).

48. A. Henderson-Sellers et al., *Bull. Am. Meteorol. Soc.* **79**, 19 (1998).

49. See "North Atlantic versus North Pacific activity" in supplemental material (54).

50. C. J. Neumann, B. R. Jarvinen, C. J. McAdie, J. D. Elms, *Tropical Cyclones of the North Atlantic Ocean, 1871–1998*. (National Climatic Center, Asheville, NC, 1999), pp. 11–15.

51. See "Disasters during low activity years" in supplemental material (54).

52. R. H. Simpson, *Weatherwise* **27**(no. 4), 169 (1974).

53. B. R. Jarvinen, C. J. Neumann, M. A. S. Davis, *NOAA Tech. Memo.*, NWS NHC 22, Miami, FL (1984).

54. Web figures 1 and 2, tables 1 and 2, and supplemental text is available at *Science* Online at www.sciencemag.org/cgi/content/full/293/5529/474/DC1.

55. D. B. Enfield, A. M. Mestas-Nuñez, *Geophys. Res. Lett.* **28**, 2077 (2001). Their study shows that the Atlantic

multidecadal fluctuations significantly influence the hydrology of the United States.

56. We thank H. Willoughby, F. Marks, J. Gamache, A. Barnston, L. Shapiro, P. Reasor, R. Rogers, R. Burpee, and M. Finke for comments on the manuscript and helpful discussions; S. Feuer and J. Harris for assistance in processing the wind data; D. Enfield for assistance with SST data and helpful suggestions; N. Dorst and S. Murillo for other technical support; S. Taylor, B. Goldenberg, and R. Simon

for editing assistance; and D. Lewis for additional helpful support. In addition, we wish to thank M. DeMaria and an anonymous reviewer for their insightful comments and N. Ward for suggestions that helped initiate this study. Partial funding for this research comes from the NOAA Office of Global Programs (Pan-American Climate Studies).

20 February 2001; accepted 8 June 2001

A Phosphatocopid Crustacean with Appendages from the Lower Cambrian

David J. Siveter,^{1*} Mark Williams,² Dieter Waloszek³

Here we describe a phosphatocopid arthropod with preserved soft anatomy from Lower Cambrian rocks of Shropshire, England, which provides evidence for the occurrence of Crustacea, including Eucrustacea, in the Early Cambrian. The find identifies an important, stratigraphically early source of well-preserved fossils (Konservat-Lagerstätte).

Most metazoan groups first appear in the fossil record during the Cambrian Period, but the nature and validity of the so-called "Cambrian Explosion" are unresolved. Some propose that cladogenic events gave rise to the metazoans in the Proterozoic [e.g., (1, 2)]. Others conclude that the Cambrian explosion is real (3). Still others maintain that in most cases the appearance of modern body plans ('crown groups'), including those of extant arthropod classes, was later than the early Cambrian (4) and favor a model of progressive diversification through the end of the Proterozoic to beyond the Cambrian.

Our material is from the Protolenus Limestone (5), which is correlated to the Toyonian Stage of Siberia (6) and is of Branchian age in terms of the Newfoundland standard for the Avalonian microplate [circa 511 million years ago (Ma); base of Cambrian circa 543 Ma] (7). The specimens are an example of "Orsten"-type preservation [e.g., (8)]; they are phosphatized and were recovered with acetic acid techniques. Phosphatocopids are a clade (9) of about 60 species of globally widespread, Lower to Upper Cambrian bivalved arthropods [see (10, 11)] that are mostly known from their purportedly primary phosphatic (12, 13) carapaces. Rare phosphatocopid specimens with preserved soft part anatomy (which has been secondarily phosphatized) are known chiefly from Upper Cambrian concretionary Orsten limestones of

Sweden (12, 13). They have also been reported from the Middle Cambrian (14) (isolated limbs only) and the Lower Cambrian (15) (two specimens, showing only the labrum and sternum).

The specimens are classified as Arthropoda, Crustacea, Phosphatocopida sp.

Material. The specimens are two carapaces, both bearing soft part anatomy [Oxford University Museum of Natural History (OUM)]. OUM A.2209 shows a labrum, sternum, and the remains of the left second, third, and fourth appendages and possibly the left first appendage; its right-side appendages are mostly obscured by matrix. OUM A.2209 bears a labrum and sternum.

Locality and stratigraphy. The fossils came from a temporary trench excavation (made by D.J.S. and M.W.), near Comley hamlet, Shropshire [Protolenus Limestone (Protolenid-Strenuelliid Biozone), Lower Comley Limestones, Comley "Series"].

Description. The subspherical shaped carapace consists of two halves ("valves") of equal size (Fig. 1, A through C); it has no hinge line or interdorsum and has a permanent gape of about 80°; its dorsal margin is 340 μm (OUM A.2209) to 330 μm (OUM A.2209) long. The doublure is well developed and is confluent with the inner lamella cuticle lining each valve.

The only visible structure that is possibly part of an antennula is a slender setulate seta on the left side of the labrum, projecting almost vertically, just below the endopod of the left second antenna (Fig. 1C). The second antenna (Figs. 1, A and D, and 2) consists of a coxa but with a gnathobasic endite carrying two or possibly three spines, a basis whose endite has two main spines flanked by four smaller spines, and an endopod consisting of three podomeres, in which the proximal podomere bears one long

¹Department of Geology, University of Leicester, Leicester LE1 7RH, UK. ²British Geological Survey, Keyworth, Nottingham NG12 5GG, UK. ³Section for Biosystematic Documentation, University of Ulm, D-89069 Ulm, Germany.

*To whom correspondence should be addressed. E-mail: djs@leicester.ac.uk